Structure and physical properties of the thermoelectric skutterudites $Eu_yFe_{4-x}Co_xSb_{12}$

A. Grytsiv and P. Rogl
Institut für Physikalische Chemie, Universität Wien, Währingerstrasse 42, A-1090 Wien, Austria

St. Berger, Ch. Paul, and E. Bauer
Institut für Festkörperphysik, T.U. Wien, Wiedner Hauptstraße 8-10 A-1040 Wien, Austria

C. Godart
CNRS-UPR209, ISCSA, 2-8 rue Henri Dunant, F94320 Thiais, France, and LURE, CNRS, Université Paris Sud, 91405 Orsay, France

B. Ni and M. M. Abd-Elmeguid
II. Physikalisches Institut, Universität Köln, Zülpicher Strasse 77, D-50937 Köln, Germany

A. Saccone and R. Ferro
Dipartimento di Chimica e Chimica Industriale, Università di Genova, Sezione di Chimica Inorganica e Metallurgica, Via Dodecaneso 31, I-16146 Genova, Italy

D. Kaczorowski
W. Trzebiatowski Institute for Low Temperature and Structure Research Polish Academy of Sciences, P-50-950 Wroclaw, P.O. Box 1410, Poland

(Received 26 October 2001; revised manuscript received 21 February 2002; published 11 September 2002)

Compounds from the solid solution $Eu_yFe_{4-x}Co_xSb_{12}$ were synthesized and found to crystallize in the partially filled skutterudite-type structure $LaFe_4P_{12}$. The maximal Eu content gradually decreases from practically full occupancy $y=0.83$ in $Eu_{0.83}Fe_4Sb_{12}$ to $y=0.44$ for $Eu_{0.44}Co_4Sb_{12}$. As a function of Fe/Co substitution in $Eu_yFe_{4-x}Co_xSb_{12}$ the magnetic transition temperature decreases from 84 K for $Eu_{0.83}Fe_4Sb_{12}$ to 8 K for $Eu_{0.44}Co_4Sb_{12}$. At lower Eu content, $Eu_{0.2}Co_4Sb_{12}$, long-range magnetic order disappears. Concomitantly, the Eu valence changes from almost divalent Eu in $Eu_{0.83}Fe_4Sb_{12}$ to $\nu\approx 2.6$ for $Eu_{0.2}Co_4Sb_{12}$. The transition metal exchange Fe/Co reduces the number of free carriers and causes a crossover of the electronic transport from a hole conductivity regime into electron dominated behavior. Thermoelectric properties change accordingly.

DOI: 10.1103/PhysRevB.66.094411 PACS number(s): 75.30.Cr, 72.15.−v, 78.70.Dm

I. INTRODUCTION

Ternary skutterudites RT_4X_{12} (R=rare earth, T=transition metal, X=P, As, Sb) form a class of attractive novel compounds, because (i) they exhibit numerous interesting physical properties and (ii) their high thermoelectric figure of merit possibly allows technical applications. For a recent review see Ref. 1. Magnetism in these compounds is determined by the electropositive filler element and, at least partly, by the transition metals. In particular, if rare earth elements are invoked, long-range magnetic order, Kondo scattering, heavy fermion behavior, and mixed and intermediate valence or pronounced crystal field splitting may be observed.

Previously, we reported on the formation, range of existence, and crystal chemistry of solid solutions $Yb_yFe_{4-x}Co_xSb_{12}$ and $Yb_yFe_{4-x}Ni_xSb_{12}$.[2,3] These materials revealed a number of outstanding low-temperature features such as intermediate valence, strongly correlated electrons, or hopping conductivity. Moreover, high Seebeck coefficients in combination with a low thermal conductivity were found. Intermediate valence in both series of compounds stem from the unstable electronic configuration (EC) of Yb, which fluctuates between the magnetic $4f^{13}$ and the nonmagnetic $4f^{14}$ ground state. In addition to Ce and Yb compounds, Eu containing materials are also known to exhibit valence instabilities. Our recent studies[4,5] on $Eu_{0.83}Fe_4Sb_{12}$, however, evidenced stable divalent Eu^{2+} as the ground state in this compound. Associated with this ground state is a total angular momentum $j=\frac{7}{2}$, and thus long-range magnetic order occurs below $T_{mag}=84$ K. The type of magnetic order could not be determined unambiguously, but spontaneous magnetization may indicate some ferromagnetic alignment of the Eu moments, or possibly, ferrimagnetism.

It is the aim of the present paper to study structural and physical properties of $Eu_yFe_{4-x}Co_xSb_{12}$ in order to follow the evolution of the EC and magnetic behavior of Eu and to probe the possibility to adjust a favorable electron/atom ratio via substitution of transition metals as well as via rare-earth defects formed as a function of $3d$ metal replacement. The formation of ternary compounds $EuFe_4Sb_{12}$ and $Eu_{0.5}Co_4Sb_{12}$ was reported earlier.[6,7] The transition metal substitution Fe/Co in $Eu_yFe_{4-x}Co_xSb_{12}$ is considered as the most promising way to optimize the thermoelectric performance of such compounds and to drive the system from *p*- to *n*-type electronic transport. This particular crossover was al-

ready demonstrated in some detail for isomorphous $Ce_yFe_{4-x}Co_xSb_{12}$, where due to the Fe/Co substitution, and concomitantly a decrease of the Ce content, transport changes from hole to electron dominated behavior.[8,9] The valence of Ce in this case, however, remains nearly constant.[10]

II. EXPERIMENTAL

A. Synthesis

Starting materials were ingots of Eu (99.9 wt %), pieces or powders of iron and cobalt (99.9 wt %) and rods of antimony (99.9 wt %). Due to the high vapor pressures of Eu and Sb at elevated temperatures, arc melting was performed under current as low as possible with repeated melting whereby the samples (about 3 g each) were flipped over and every second time were fragmented into several pieces, the outer parts moved to inside positions prior to remelting. With this method and compensating the losses of evaporation by additional Eu and Sb a dense product was achieved. The samples were then sealed under vacuum in silica capsules, slowly heated (50 °C/h) to a range of 600 to 750 °C and held for up to 150 h followed by quenching in water. As rare-earth-iron-based skutterudite phases do not form directly from the melt, single-phase products can only be obtained after long-term annealing of the samples. The pellets were found to be homogeneous with only minor amounts of secondary phases (<2 vol %). Sample composition of $Eu_{0.42}FeCo_3Sb_{12}$ used for Mössbauer and x-ray absorption spectroscopy, as checked by wet chemical analysis, was in agreement with the composition determined from x-ray Rietveld refinement and electron microprobe analysis.

B. Electron microprobe analysis

Light optical microscopy (LOM) on selected compounds, which were polished and etched by standard methods, scanning electron microscopy, and electron microprobe (EPMA) analyses based on energy dispersive x-ray spectroscopy [Si(Li) detector] were used to examine equilibrium compositions. For quantitative EPMA the samples were analyzed employing an accelerating voltage of 20 kV for a counting time of 100 sec. X-ray energy spectra (Eu-L_α, Fe-K_α, Co-K_α, and Sb-L_α) were processed using the ZAF-4/FLS software package supplied by Link Systems, Ltd., England. A peak from a pure cobalt standard was used in a calibration procedure to monitor beam current, gain and resolution of the spectrometer. Pure elements and a $EuMg_2$ master alloy served as standards to carry out the deconvolution of overlapping peaks and background subtraction. Finally, the x-ray intensities were corrected for atomic number, absorption, and fluorescence effects using the TIMI program.[11]

C. X-ray powder diffraction

X-ray powder diffraction data were obtained using a Huber Guinier powder camera and monochromatic Cu$K\alpha_1$ radiation with an image plate recording system. Precise lattice parameters were calculated by least squares fits to the indexed 4Θ values obtained from x-ray film recordings using Ge as internal standard ($a_{Ge}=0.5657906$ nm). For quantitative refinement of the atom positions, x-ray intensities were collected in transmission from a flat specimen in a Guinier image plate camera. Rietveld refinements employed the FULLPROF program[12] on the basis of our single crystal data of $YbFe_4Sb_{12}$.[13]

D. EuL_{III} x-ray absorption and ^{151}Eu Mössbauer spectroscopies

L_{III} measurements were performed at the French synchrotron radiation facility (LURE) in Orsay using the x-ray beam of the DCI storage ring (working at 1.85 GeV and ~320 mA) on the EXAFS D21 station. A double Si 311 crystal was used as a monochromator. The rejection of third order harmonics was achieved with the help of two parallel mirrors adjusted to cutoff energies higher than ~10 keV. Experiments were carried out in the energy range 6900 eV to 7080 eV, which contains the L_{III} edge of Eu. Samples finely powdered in a glove box were spread on an adhesive Kapton tape and four such tapes were stacked in a row in order to ensure a good signal. X-ray absorption spectra were measured at two fixed temperatures 300 and 10 K.

^{151}Eu Mössbauer effect (ME) measurements were performed using a 100 mCi SmF_3 Mössbauer source at 300 and 4.2 K. During the measurements, source and absorber were kept at the same temperature in a He cryostat.

E. Magnetic and transport properties

A superconducting quantum interference device (SQUID) magnetometer served for the determination of the magnetization from 2 up to 300 K in fields up to 6 T. The electrical resistivity of bar shaped samples was measured using a four probe dc method in the temperature range from 0.4 K to room temperature and fields up to 12 T. A liquid pressure cell with paraffin oil as pressure transmitter served to generate hydrostatic pressure up to about 1.6 GPa. The absolute value of the pressure was determined from the superconducting transition temperature of lead.[14] Thermal conductivity measurements were performed in a flow cryostat on cuboid-shaped samples (length: about 1 cm, cross section: about 2–3 mm^2), which were kept cold by anchoring one end of the sample onto a thick copper panel mounted on the heat exchanger of the cryostat. The temperature difference along the sample, established by electrical heating, was determined by means of a differential thermocouple (Au+0.07% Fe/Chromel). The measurement was performed under high vacuum and three shields mounted around the sample reduced the heat losses due to radiation at finite temperatures. The innermost of these shields is kept on the temperature of the sample via an extra heater maintained by a second temperature controller. Thermopower measurements were carried out with a differential method. The absolute thermopower $S_x(T)$ was calculated using the following equation: $S_x(T)=S_{Pb}(T)-V_{Pb/x}/\Delta T$ where S_{Pb} is the absolute thermopower of lead and $V_{Pb/x}$ is the thermally induced voltage across the sample, depending on the temperature difference ΔT.

TABLE I. Sample preparation, crystallographic and electron microprobe data for $Eu_yFe_{4-x}Co_xSb_{12}$ compounds.

Accepted composition	Heat treatment	Composition: X-ray analysis	Composition: Data from EMPA Eu-Fe-Co-Sb in at. %	Lattice Parameters a [nm]
$Eu_{0.83}Fe_4Sb_{12}$	600 °C (4 days)	$Eu_{0.83}Fe_4Sb_{12}$	$Eu_{0.90}Fe_4Sb_{12}$ 5.3-23.5-0-71.2	0.91657(7)
$Eu_{0.75}Fe_4Sb_{12}$	600 °C (2 days)	$Eu_{0.75}Fe_4Sb_{12}$	-	0.91628(8)
$Eu_{0.75}Fe_{3.5}Co_{0.5}Sb_{12}$	650 °C (5 days)	$Eu_{0.75}Fe_{3.5}Co_{0.5}Sb_{12}$	$Eu_{0.84}Fe_{3.52}Co_{0.48}Sb_{12}$ 4.96-20.6-2.8-71.7	0.91537(7)
$Eu_{0.75}Fe_{3.1}Co_{0.9}Sb_{12}$	600 °C (2 days)	$Eu_{0.75}Fe_3CoSb_{12}$	$Eu_{0.80}Fe_{3.1}Co_{0.9}Sb_{12}$ 5.1-17.8-5.3-71.7	0.91428(9)
$Eu_{0.77}Fe_{2.9}Co_{1.1}Sb_{12}$	600 °C (4 days) +650 °C (3 days)	$Eu_{0.77}Fe_3CoSb_{12}$	$Eu_{0.87}Fe_{2.9}Co_{1.1}Sb_{12}$ 5.15-16.8-6.4-71.6	0.91457(9)
$Eu_{0.63}Fe_{2.4}Co_{1.6}Sb_{12}$	600 °C (8 days) +650 °C (5 days)	$Eu_{0.63}Fe_{2.5}Co_{1.5}Sb_{12}$	$Eu_{0.59}Fe_{2.4}Co_{1.6}Sb_{12}$ 3.5-13.8-9.1-73.5	0.91257(9)
$Eu_{0.7}Fe_2Co_2Sb_{12}$	600 °C (6 days) +sintering 650 °C (4 days)	$Eu_{0.7}Fe_2Co_2Sb_{12}$	Heterogeneous	0.91150(2)
$Eu_{0.42}FeCo_3Sb_{12}$[a]	600 °C (6 days) +650 °C (3 days)	$Eu_{0.42}FeCo_3Sb_{12}$	$Eu_{0.46}FeCo_3Sb_{12}$ 2.7-17.3-6.1-73.8	0.90851(7)
$Eu_{0.42}Fe_{0.6}Co_{3.4}Sb_{12}$	600 °C (14 days) +650 °C (14 days)	$Eu_{0.42}Fe_{0.5}Co_{3.5}Sb_{12}$	$Eu_{0.44}Fe_{0.6}Co_{3.4}Sb_{12}$ 2.63-3.6-19.7-73.9	0.90819(4)
$Eu_{0.44}Co_4Sb_{12}$	650 °C (7 days) +750 °C (7 days)	$Eu_{0.44}Co_4Sb_{12}$	$Eu_{0.60}Co_4Sb_{12}$ 3.5-23.4-73.1	0.90934(2)
$Eu_{0.2}Co_4Sb_{12}$	sintering 650 °C (30 days) +750 °C (7 days)	$Eu_{0.2}Co_4Sb_{12}$	$Eu_{0.21}Co_4Sb_{12}$ 1.21-24.0-74.8	0.90608(5)
$Co_4Sb_{12}(CoSb_3)$	sintering 700 °C (4 days)	$CoSb_3$		0.90368(2)

[a] $Eu_{0.43}Fe_{0.98}Co_{3.07}Sb_{12}$ from wet chemical analysis.

III. RESULTS AND DISCUSSION

A. Structural chemistry

All x-ray powder diffraction patterns were indexed on the basis of a body-centered cubic lattice (see Table I) suggesting isotypism with $LaFe_4P_{12}$.[15] The refinements of the x-ray intensities (Rietveld refinements; see Table II) in all cases converged satisfactorily for a fully ordered atom arrangement with respect to the atom site distribution among Eu, (Fe, Co), and Sb atoms. Due to their close chemical alloying behavior iron and cobalt atoms were assumed in a random occupation of the transition metal sites in $8c$ of space group $Im\bar{3}$-T_h^5. Occupation factors were refined and corresponded to a full occupancy of the Fe/Co and the Sb sublattice, however, revealed considerable defects in the Eu site in strong dependence on the amount of the Fe/Co concentration. Preferred orientation was taken into account for all refinements, but was found to be negligibly small. The final Eu content of the compounds was evaluated from the combined data obtained from Rietveld refinements and electron microprobe measurements EPMA. The latter technique also served to monitor the proper Fe/Co content in the compounds. Only minor shifts with respect to the nominal starting composition of the samples were detected (see Table I). These investigations confirmed a systematic trend for the maximal Eu occupancy in the parent lattice: starting from almost complete occupation of the Eu site in $Eu_yFe_4Sb_{12}$ a gradual decrease of the Eu content is observed with increasing Co content of the sample. The Eu content runs from $0.75<y<0.83$ in $Eu_yFe_4Sb_{12}$ to $0<y<0.44$ for $Eu_yCo_4Sb_{12}$. The observed trend is in line with that for the homologous series $Ce_yFe_{4-x}Co_xSb_{12}$.[8] Due to the usually strong correlation with isotropic temperature factors B_{iso}, the occupancies were kept fixed in the final runs to refine the B_{iso} values. The results of the refinements are summarized in Table II also including interatomic distances, which reveal the general bonding situation in intermetallic skutterudite phases as, e.g., discussed in Ref. 15. In a first analysis thermal parameters for the Eu atoms turn out to be rather small, however, after employing a new correction for asymmetric peak shape converged towards physically acceptable values. Thermal displacement parameters as derived from x-ray powder diffraction generally hamper from strong correlation with occupancies and furthermore tend to subsume influences from peak shape, absorption, etc., and therefore should not be overinterpreted. The variation of the lattice parameters as a function of the Fe/Co exchange and the dependency from the Eu content is shown in Fig. 1, where solid lines, as a guide to the eye, denote the unit cell dimensions for maximum and minimum Eu contents in the compounds.

TABLE II. Structural data (Rietveld refinements) for $Eu_yFe_{4-x}Co_xSb_{12}$ ($LaFe_4Fe_4P_{12}$ type, space group Im-3; No. 204).

Parameter/compound	$Eu_{0.75}Fe_{3.5}Co_{0.5}Sb_{12}$	$Eu_{0.63}Fe_{2.4}Co_{1.6}Sb_{12}$	$Eu_{0.42}Fe_{0.6}Co_{3.4}Sb_{12}$
a [nm]	0.91537(7)	0.91257(9)	0.90819(4)
Reflections measured (Θ range)	84 ($8 \leqslant 2\Theta \leqslant 100$)	84 ($8 \leqslant 2\Theta \leqslant 100$)	81 ($8 \leqslant 2\Theta \leqslant 100$)
Number of variables	28	25	20
$R_F = \Sigma\lvert F_0 - F_c\rvert / \Sigma F_0$	0.040	0.050	0.070
$R_I = \Sigma\lvert I_0 - I_c\rvert / \Sigma I_0$	0.046	0.050	0.072
$R_{wP} = [\Sigma w_i \lvert y_{oi} - y_{ci}\rvert^2 / \Sigma w_i \lvert y_{oi}\rvert^2]^{1/2}$	0.060	0.036	0.048
$R_p = \Sigma\lvert y_{0i} - y_{ci}\rvert / \Sigma\lvert y_{0i}\rvert$	0.031	0.027	0.034
$R_c = [(N-P+C)/\Sigma w_i y_{oi}^2)]^{1/2}$	0.020	0.019	0.018
$\chi^2 = (R_{wP}/R_c)^2$	8.67	3.52	7.19
	Atom parameters		
Eu in 2*a* (0,0,0), occ.	0.751(6)	0.632(3)	0.418(4)
$B_{iso} \times 10^2$ [nm^2]	0.97(2)	1.01(3)	0.84(2)
M in 8*c* (1/4,1/4,1/4)	7Fe+1Co	5Fe+3Co	1Fe+7Co
$B_{iso} \times 10^2$ [nm^2]	0.44(1)	0.53(1)	0.51(1)
Sb in 24*g* (0,*y*,*z*) *y*:	0.15977(8)	0.15918(5)	0.15869(6)
z:	0.33730(7)	0.33685(4)	0.33593(6)
$B_{iso} \times 10^2$ [nm^2]	0.69(1)	0.63(1)	0.57(2)
Interatomic distances [nm]; standard deviations generally <0.0005 nm			
Eu-12 Sb	0.3416	0.3400	0.3374
Eu-8 M	0.3964	0.3952	0.3933
M-6 Sb	0.2561	0.2553	0.2540
M-2 Eu	0.3964	0.3952	0.3933
Sb-2 M	0.2561	0.2553	0.2540
Sb-1 Sb	0.2979	0.2978	0.2980
Sb-1 Sb	0.2925	0.2905	0.2882
Sb-1 Eu	0.3416	0.3400	0.3374

B. Eu-valence and magnetism

To determine the valence state and thus the magnetic behavior of the Eu ion in $Eu_yFe_{4-x}Co_xSb_{12}$, L_{III} absorption edge measurements were performed at room temperature and at $T = 10$ K, respectively. Results are shown in Fig. 2(a). The absorption spectra obtained are characterized by a double peak structure, evidencing noninteger valence of the Eu ions throughout the series. Spectral weight is centered around $E_1 = 6973$ eV and $E_2 = 6982$ eV, with no substantial dependence on the particular compound. While the former peak is associated with the 2+ state of Eu, the latter corresponds to Eu^{3+}. These states can be identified with a total angular momentum $j = \frac{7}{2}$ and $j = 0$, respectively. The magnetic behavior therefore varies between a stable magnetic state, yielding an effective magnetic moment $\mu_{eff} = 7.93\mu_B$ and a nonmagnetic ground state with $\mu_{eff} = 0$, respectively. Eu^{2+} resembles the magnetic properties of Gd^{3+}, which are characterized by the absence of an orbital contribution to the total angular momentum *j*, thus $j = s = \frac{7}{2}$. In such a particular case, crystal-field effects are absent in physical properties and $j = \frac{7}{2}$ acts in the whole temperature range. Results of a standard analysis[16] of the present L_{III} data are summarized in Fig. 2(b). Three key features, (i) to (iii), are deduced from the present L_{III} spectra for $Eu_yFe_{4-x}Co_xSb_{12}$. (i) The Eu valence changes from $\nu = 2.25$ ($Eu_{0.83}Fe_4Sb_{12}$) to $\nu = 2.59$ ($Eu_{0.2}Co_4Sb_{12}$) as a response to the Fe/Co substitution. The almost linear relationship, valency vs Eu content, indicates that the valency depends primarily on the changing Eu content. This is particularly seen in $Eu_yCo_4Sb_{12}$ ($y = 0.2, 0.44$) where the higher Eu content favors a lower Eu valency. Since the maximum Eu content is controlled by the extent of the Fe/Co substitution (see Fig. 1), a corresponding valence dependency ν_{Eu} vs x_{Co} is obvious. Although for the homologous series $Ce_yFe_{4-x}Co_xSb_{12}$ the Ce content *y* decreases significantly with x_{Co}, the cerium valency remains unaffected by the Fe/Co substitution.[10] This behavior contrasts the Eu valence dependency in $Eu_yFe_{4-x}Co_xSb_{12}$. Significant deviations from the 2+ state are usually accounted for in terms of intermediate valence, however, the Fe/Co substitution on a microscopic scale may be resolved in Fe-rich T_4Sb_{12} units with almost divalent Eu (as in $Eu_{0.83}Fe_4Sb_{12}$; the structure is practically filled and the compound is magnetic) and in Co-rich T_4Sb_{12} units, where the effect of Eu vacancy may drive the compound more towards the nonmagnetic state. The

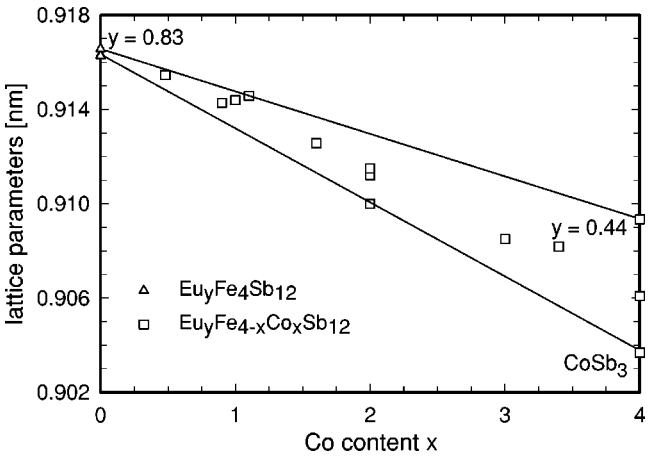

FIG. 1. Dependency of lattice parameters throughout the series $Eu_yFe_{4-x}Co_xSb_{12}$; the solid lines are a guide to the eye denoting the unit cell dimensions for maximum and minimum Eu content in the compounds.

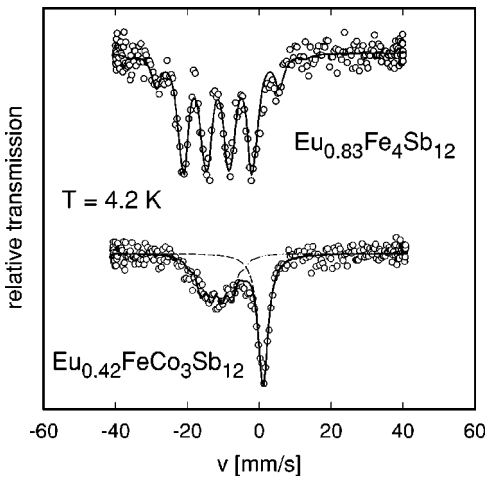

FIG. 3. ^{151}Eu Mössbauer spectra of $Eu_{0.83}Fe_4Sb_{12}$ and $Eu_{0.42}FeCo_3Sb_{12}$ collected at 4.2 K. Solid lines are least squares fits to the data. Dashed and dashed-dotted lines refer to contributions of Eu^{3+} and Eu^{2+}, respectively.

double random substitution Fe/Co and Eu/vacancy on the macroscopic scale may thus result in a simple average mix of the two Eu valence states. (ii) No temperature-dependent changes of spectral weight occur for both electronic configurations in the whole series. Consequently, the nonmagnetic state, associated with the trivalent behavior, is located well above the ground state. Thermal energy proportional to room temperature does not significantly change the population of this excited level. In the case of intermediate valence, however, a pronounced temperature dependence is expected[17] and is observed in many noninteger valent Eu compounds.[18] (iii) In each case, the energy separation ΔE between both absorption maxima is larger than 8 eV, independent of temperature and almost independent of the concentration. In contrast, typical intermediate valence systems based on Eu exhibit ΔE below this value.[19–22] These experimental facts obviously indicate that $Eu_yFe_{4-x}Co_xSb_{12}$ is characterized by some sort of mixed valence behavior.

There is always a certain probability for the occurrence of the so-called ''shake-up'' effect:[23] after the creation of the $2p$ core hole in the fully relaxed final state, the number of $4f$ electrons is lowered with respect to that of the fully undisturbed ground state due to the partial promotion of a $4f$ electron into the conduction band. This effect was frequently considered to explain L_{III} data, providing a slight, but non-negligible correction of L_{III} valences, which generally appear to be overestimated with respect to corresponding data obtained from Mössbauer spectroscopy. Applied to our case, the strength of the ''shake-up'' effect seems to depend on Fe/Co substitution concomitant with Eu/vacancy distribution. It is interesting to point out here that in $Ce(Fe,Co)_4Sb_{12}$ (Ref. 10) Ce is trivalent and the broadening of the L_{III} edge occurs from e_g-t_{2g} splitting of the conduction band (final state of the L_{III} edge transition), whereas in $YbFe_4Sb_{12}$ intermediate valence has been reported.[13] In $Eu_yFe_{4-x}Co_xSb_{12}$ mixed valence with dominant effects of two local environments of the Eu ions is seen, differing in the Fe/Co concentration (see also below).

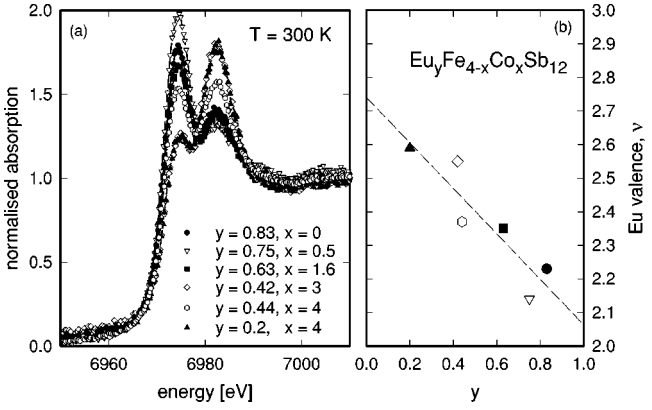

FIG. 2. (a) Energy dependence of the L_{III} absorption edge spectra for various concentrations of $Eu_yFe_{4-x}Co_xSb_{12}$ measured at $T=300$ K. (b) Valence ν of Eu as derived from L_{III} spectra.

Mössbauer measurements were performed on $Eu_{0.83}Fe_4Sb_{12}$ and $Eu_{0.42}FeCo_3Sb_{12}$ at room temperature and 4.2 K. Results are compared in Fig. 3 for $T=4.2$ K. As previously reported,[5] $Eu_{0.83}Fe_4Sb_{12}$ revealed just a single resonance line in the paramagnetic state corresponding to an isomer shift (IS)$=-11.7$ mm/s, indicating an almost divalent nature of the Eu ion. This Eu^{2+} line splits magnetically at 4.2 K due to the ordering of the Eu^{2+} moments at low temperatures ($T_{\mathrm{mag}}=84$ K). The value of the effective magnetic hyperfine field is $B_{\mathrm{eff}}=-23.8$ T. In the case of $Eu_{0.42}FeCo_3Sb_{12}$ one encounters distinct differences: as shown in Fig. 3 a second line appears at IS$=0$ mm/s (Eu^{3+}), inferring a mixed valence state with a ratio of $Eu^{2+}/Eu^{3+}=1$, in fine agreement with the above mentioned L_{III} data ($\nu=2.55$). This result excludes any dynamic valence fluctuations within this series. As expected, the Eu^{2+} component of the spectrum of $Eu_{0.42}Fe_4Sb_{12}$ is magnetically split due to the ordering of the Eu^{2+} moments and results in a $B_{\mathrm{eff}}=-11(2)$ T. This value is about two times smaller than that of $Eu_{0.83}Fe_4Sb_{12}$ and can be explained as follows: a reduction of the Eu concentration by about a factor of 2 causes a corre-

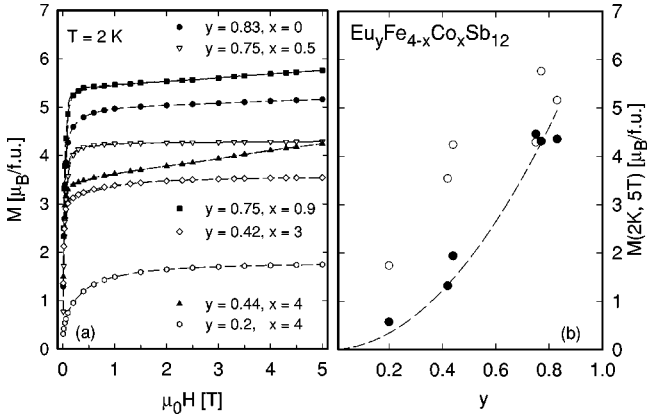

FIG. 4. (a) Isothermal magnetization M vs field $\mu_0 H$ for various concentrations of $Eu_yFe_{4-x}Co_xSb_{12}$ measured at $T=2$ K. (b) Magnetization of $Eu_yFe_{4-x}Co_xSb_{12}$ at 5 T and 2 K (open circles) and calculated contribution of Eu (filled circles).

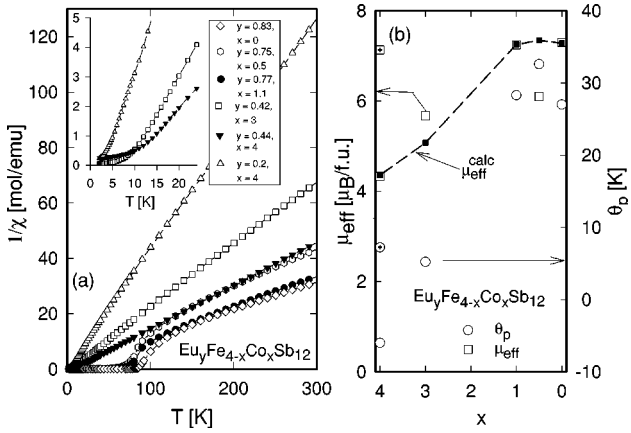

FIG. 5. (a) Temperature-dependent inverse magnetic susceptibility $1/\chi$ of $Eu_yFe_{4-x}Co_xSb_{12}$ for various concentrations x. The inset shows the low temperature behavior for selected samples. (b) Effective magnetic moment $\mu_{\rm eff}$ and paramagnetic Curie temperature θ_p of $Eu_yFe_{4-x}Co_xSb_{12}$; symbols labeled with crosses refer to $x=4$, $y=0.44$.

sponding decrease in the number of the magnetic neighboring ions and thereby a reduction of their contribution to $B_{\rm eff}$ (transferred hyperfine field).[24] In this respect, it is interesting to note the giant value, $B_{\rm eff}=-67$ T, previously reported for $EuFe_4P_{12}$ (Ref. 25) and attributed to a substantial $4f$-$5d$ band mixing. In addition, such type of band coupling leads to a reduction of the Eu^{2+} moment ($6.2\mu_B$) and to an increase in the IS (-6.0 mm/s).[25] As mentioned above, this is not the case in our samples. Band structure calculations (full potential linearized plane wave method[26]) show a significantly larger d-p and s-f mixing for RFe_4P_{12} than for RFe_4Sb_{12}, suggesting that the electronic states [Fe($3d$), Sb($5p$), and Eu($5d$)] are more localized than in the case of $EuFe_4P_{12}$. This observation is also consistent with the trend in the volume of the unit cell which for $Eu_{0.83}Fe_4Sb_{12}$ is about 37% larger than that of $EuFe_4P_{12}$.

Isothermal magnetization measurements in fields ranging from 0.01 to 5 T [Fig. 4(a)] exhibit spontaneous magnetization for each of the investigated compounds except for $Eu_{0.2}Co_4Sb_{12}$. The latter, however, saturates already at external fields of about 2 T. These experimental findings exclude antiferromagnetic order throughout the series. Figure 4(b) summarizes the magnetization measured at 2 K and 5 T as a function of the Eu content per formula unit (open circles). Employing the particular Eu content and the respective Eu valence of the compound we arrive at the magnetization associated with the Eu ion at 5 T [filled circles in Fig. 4(b)]. The difference between the measured magnetization and the Eu contribution is attributed to the $[(Fe,Co)_4Sb_{12}]$ sublattice. As seen from Fig. 4(b), these values vary between 0.2 and $0.6\mu_B$ per (Fe,Co) atom. A spontaneous magnetization per Fe atom of this order of magnitude was recently encountered in a neutron diffraction study of ferromagnetic $Nd_{0.72}Fe_4Sb_{12}$ ($\mu_{\rm Fe}=0.26\mu_B$).[27] The additional moment derived for the $[(Fe,Co)_4Sb_{12}]$ sublattice seems to be a result of the molecular field associated with ferromagnetically ordered Eu ions. As mentioned above, this particular feature is found in ferromagnetic $Nd_{0.72}Fe_4Sb_{12}$, but appears to be absent in magnetically nonordered compounds such as $Ce_yFe_{4-x}Co_xSb_{12}$ (Ref. 28) as well as $YbFe_4Sb_{12}$.[13]

Shown in Fig. 5(a) is the inverse magnetic susceptibility $1/\chi(T)$ of $Eu_yFe_{4-x}Co_xSb_{12}$ as a function of temperature. The significant deviation of $1/\chi$ from linearity below 100 K ($x=0$) and the s-shaped temperature dependence is reminiscent of ferrimagnetic order with a phase transition temperature decreasing from $T_{\rm mag}=84$ K for $x=0$, $y=0.83$ to $T_{\rm mag}=0$ for $x=4$, $y=0$, and 0.2. Moreover, as the Co content increases upon substitution, the characteristic signature of the phase transition in $1/\chi$ becomes weaker since the Eu content lowers simultaneously. However, if the Eu content is increased from $y=0.2$ to $y=0.44$ in the case of $x=4$, long-range magnetic order appears again below $T_{\rm mag}=8$ K [compare inset, Fig. 5(a)]. Both latter observations indicate that the ordered ground state is primarily stabilized by Eu. In the case of $y=0.44$, the Ruderman-Kittel-Kasuya-Yosida interaction might account for the observed long-range magnetic order, whereas for $y=0.2$, the high content of vacancies at the Eu site prevents long-range magnetic order.

In order to derive the effective magnetic moment $\mu_{\rm eff}$, the Curie constant C, the paramagnetic Curie temperature θ_p, and a temperature-independent susceptibility contribution χ_0 from the experimental susceptibility data, least squares fits according to a modified Curie-Weiss law $\chi(T)=\chi_0+C/(T-\theta_p)$ were applied to $\chi(T)$ above about 120 K. Results of this procedure are shown in Fig. 5(b). The effective moments obtained, range from 7.3 to $4.3\mu_B$ and the paramagnetic Curie temperature from 27 to -6 K for $x=0$ to $x=4$, respectively. The latter indicates a crossover from a ferromagnetic type of interaction between moments to an antiferromagnetic type, driven by the Fe/Co substitution. The slightly different paramagnetic data of $Eu_{0.83}Fe_4Sb_{12}$, as reported in Refs. 4, 5, are attributed to different sample preparation procedures. The measured total effective magnetic moment of a particular compound consists of two components coming from the Eu sublattice as well as from $[(Fe,Co)_4Sb_{12}]$. Measurements of e.g., isomorphous $La_{0.83}Fe_4Sb_{12}$ and $Ca_{0.83}Fe_4Sb_{12}$,[6] where the electropositive element is nonmagnetic, reveal ef-

fective magnetic moments $\mu_{\text{eff}}=3.0\mu_B$ and $\mu_{\text{eff}}=3.7\mu_B$, respectively, which primarily are associated with the $3d$ magnetism of Fe. Measurements carried out on $Pr_{0.73}Fe_4Sb_{12}$ and $Nd_{0.72}Fe_4Sb_{12}$ (Ref. 27) revealed total effective moments of $4.19\mu_B$ and $4.44\mu_B$, respectively. Assuming theoretical rare earth moment values in combination with the 80% occupancy of the voids, yields again significant values of the effective magnetic moments of $[Fe_4Sb_{12}]$ of $\mu_{\text{eff}}=2.7\mu_B$ and $\mu_{\text{eff}}=3.1\mu_B$, respectively. A recent study performed on $Co_{1-x}Fe_xSb_3$ (Ref. 29) demonstrated the development of a paramagnetic moment on an increasing Fe content, approaching $1.73\mu_B$/Fe atom. This value is consistent with trivalent iron in a low-spin d^5 electronic configuration with a net spin $s=\frac{1}{2}$ and consequently $\mu_{\text{eff}}=2[s(s+1)]^{1/2}\approx 1.73\mu_B$. In contrast, $CoSb_3$ contains no unpaired spins of free electrons and therefore behaves diamagnetically. A comparison of the ternary with the binary skutterudites evidences that the electropositive filler elements, independent of their magnetic state, enhance magnetism of the $(Fe,Co)_4Sb_{12}$ sublattice, obviously inferred by non-negligible changes of the electronic structure.[30]

To analyze the paramagnetic behavior within the series $Eu_yFe_{4-x}Co_xSb_{12}$ we first deal with the end members $x=0$ and $x=4$. Assuming for $Eu_{0.83}Fe_4Sb_{12}$ that $\mu_{\text{eff}}(\text{meas.})=7.30\mu_B=(y[\mu_{\text{eff}}(\text{Eu})]^2+\{\mu_{\text{eff}}[(Fe,Co)_4Sb_{12}]\}^2)^{1/2}$ and assigning $\mu_{\text{eff}}(\text{Eu})=\mu_{\text{eff}}(\text{Eu}^{2+})(3-\nu)^{1/2}$ as the effective moment of Eu, we arrive at $\mu_{\text{eff}}([Fe_4Sb_{12}])=3.76\mu_B$, a value reasonably close to that derived for isomorphous $La_{0.83}Fe_4Sb_{12}$ or $Ca_{0.83}Fe_4Sb_{12}$.[6] The case of low Eu content $y=0.2$ corresponds to a Eu valency of $\nu=2.59$ as obtained from L_{III} data. The effective moment compatible with ν thus amounts to $5.08\mu_B$. To match the experimental total effective moment of $4.33\mu_B$ causes a magnetic contribution of $3.69\mu_B$ for the Co_4Sb_{12} sublattice, which is slightly lower than the value obtained above for the homologous Fe_4Sb_{12} sublattice. An analogous procedure for $Eu_{0.44}Co_4Sb_{12}$ yields an effective moment of $5.81\mu_B$. The observation that a paramagnetic moment is derived for $[Co_4Sb_{12}]$ in $Eu_yCo_4Sb_{12}$, in contrast to binary diamagnetic $CoSb_3$, implies again a substantial change of the electronic band structure in filled skutterudites.

The variation of the effective moment as a function of the Fe/Co exchange throughout the series should follow a simple combination of the two major contributions: (i) the $[(Fe,Co)_4Sb_{12}]$ unit (taken as constant, $3.76\mu_B$) and (ii) the paramagnetism of Eu, according to its concentration per formula unit and its correspondent valence, both varying as a function of the Fe/Co exchange. The concentration dependence of the effective moment, calculated on the basis of these two contributions follows roughly the measured curve. In order to account for the effective magnetic moment with respect to both, the Fe/Co substitution and the simultaneous Eu incorporation, the following model is proposed: starting with diamagnetic $[Co_4Sb_{12}]$ and low spin $[Fe_4Sb_{12}]$, the Eu electrons are transferred in such a way that the proportional number per Fe/Co atom creates unpaired Co spins but diminishes the magnetic effect of the unpaired Fe spins. The moments calculated in this manner are generally somewhat low, but the shape of the concentration dependency roughly follows the experimental curve. Such an analysis indicates that upon Fe/Co substitution the effective magnetic moment of $[(Fe,Co)_4Sb_{12}]$ does not vanish, even in the case of iron-free $[Co_4Sb_{12}]$. The latter appears to be in disagreement to diamagnetic $CoSb_3$.[29] Band structure calculations, however, evidence that the electronic structure of binary skutterudites can deviate significantly from that of filled skutterudites[30] and consequently, differences in the magnetic state can occur. Although our model may be too simple, a strong impact of the Eu atoms can be made responsible for the discrepancy between the calculated and the experimental paramagnetic moments and furthermore driving a paramagnetic contribution in $[Co_4Sb_{12}]$.

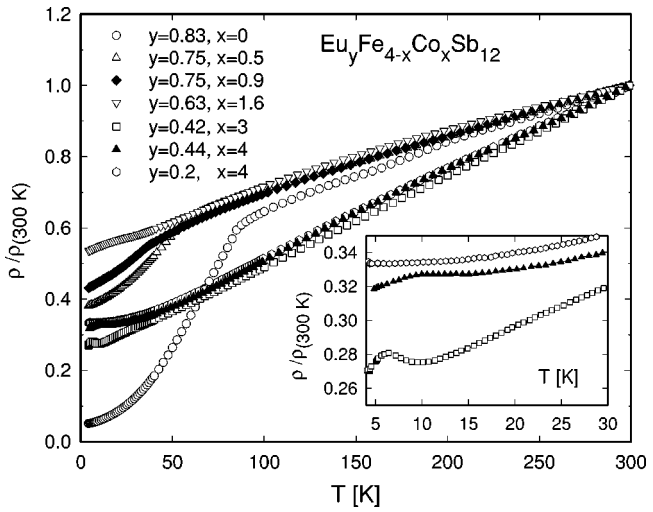

FIG. 6. Temperature-dependent electrical resistivity ρ of $Eu_yFe_{4-x}Co_xSb_{12}$ for various concentrations x, plotted in a normalized representation. The inset shows the low-temperature behavior for selected samples.

C. Transport properties

The temperature-dependent electrical resistivity $\rho(T)$ is plotted in Fig. 6 in a normalized representation for a number of specimens of $Eu_yFe_{4-x}Co_xSb_{12}$. The absolute resistivity at room temperature can reach values above 1 mΩ cm, partly due to the mechanical quality of the sample (microcracks, pores, etc.) and partly due to crystallographic disorder of (Fe/Co) on the $8c$ sites of the unit cell. Overall resistivity values of ordered ternary $Eu_yFe_4Sb_{12}$ as well as of $Eu_yCo_4Sb_{12}$, however, can be well below this limit.[5,31] As already inferred from the magnetic measurements, the transition temperature T_{mag} decreases with a growing content of Co. This follows also clearly from the $\rho(T)$ data, where a kink in the vicinity of T_{mag} moves to lower temperatures. However, for x values roughly larger than 2, a local minimum, slightly above T_{mag}, develops. Minima in $\rho(T)$ above magnetic ordering are frequently found in both ferromagnetic and antiferromagnetic materials.[32] While the former may be associated with strong spin fluctuations, the latter results from a change in the Fermi surface brought about by the new superlattice boundaries due to antiferromagnetic or-

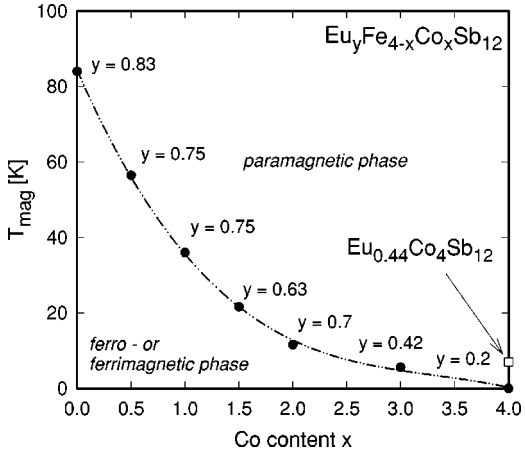

FIG. 7. Concentration-dependent ordering temperatures for $Eu_yFe_{4-x}Co_xSb_{12}$.

dering. However, since antiferromagnetic ordering can be excluded in this series, the substitution of Fe by Co seems to be responsible for the appearance of such spin fluctuation effects. It is well known that rare earth intermetallic compounds containing Co often exhibit distinctive spin fluctuation effects. Concentration dependent ordering temperatures, using susceptibility and resistivity data are outlined in Fig. 7.

Interesting features were also deduced from pressure dependent resistivity measurements performed for compounds richest in Fe ($x=0$,$x=0.5$) and for $Eu_{0.44}Co_4Sb_{12}$ up to about 1.6 GPa (see Fig. 8). The overall behavior of $\rho(T)$ of $Eu_{0.75}Fe_4Sb_{12}$ and $Eu_{0.75}Fe_{3.5}Co_{0.5}Sb_{12}$ shows a decrease of the absolute resistivity values as well as an increase of the transition temperature T_{mag}. The decrease in resistivity also causes a decrease of the spin-disorder contribution to the total measured effect which can be derived via Matthiessen's rule according to $\rho(T)=\rho_0+\rho_{ph}(T)+\rho_{spd}$, where the subscripts 0, ph, and spd refer to interactions of the conduction electrons with static imperfections, phonons, and magnetic moments, respectively. In the paramagnetic temperature range, the latter is temperature independent since crystal field splitting is absent in this series of compounds. Experimentally, ρ_{spd} follows from an extrapolation of the high-

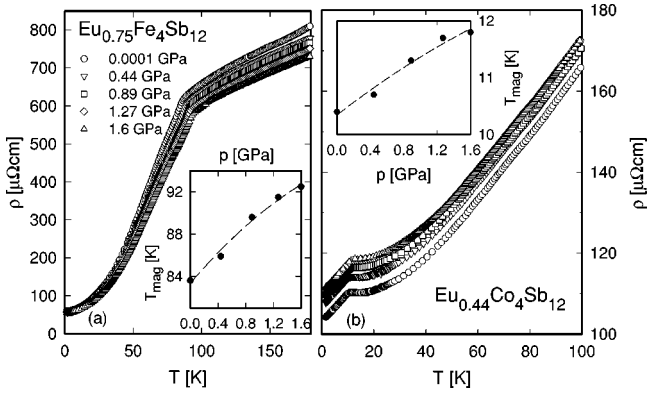

FIG. 8. Temperature-dependent electrical resistivity ρ of (a) $Eu_{0.75}Fe_4Sb_{12}$ and (b) $Eu_{0.44}Co_4Sb_{12}$ for various values of applied pressure.

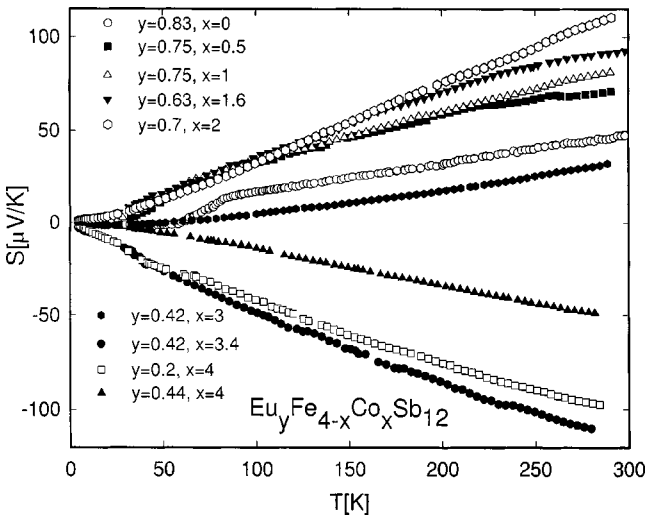

FIG. 9. Temperature-dependent thermopower S of $Eu_yFe_{4-x}Co_xSb_{12}$ for various concentrations x.

temperature part of $\rho(T)$ towards zero. The spin-disorder contribution ρ_{spd} depends on the total angular momentum of Eu, on the exchange coupling constant J, the Landé factor g, and on the effective carrier mass m^*.[32] The observed decrease of ρ_{spd} upon pressure may indicate both a decrease of J due to the mutual approach of the magnetic ions and/or a decrease of the effective carrier mass m^*. However, when comparing this result with the specimen richest in Co, i.e., $Eu_{0.44}Co_4Sb_{12}$, a remarkably different response to pressure is derived, namely an overall increase of the resistivity and thus an increase of ρ_{spd}. This mirrorlike behavior with respect to the Fe rich compound most likely is a consequence of the change of the carrier type, from holelike for the former to electronlike for the latter.

The phase transition temperature for $x=0$ ($y=0.75$) and $x=4$ ($y=0.44$) increases with $dT_{mag}/dp=5.85$ and 0.95 K/GPa, respectively, giving rise to a Grüneisen constant $\Gamma=B_0/T_{mag}\ dT_{mag}/dp$ of 6.7 and 9.6, for $x=0$ and $x=4$, respectively, if the bulk modulus B_0 is assumed to be $B_0=100$ GPa. The latter is some average value deduced for intermetallic compounds with Eu.[33] The increase of T_{mag} upon pressure and the magnitude of the observed values of Γ are usually intrinsic properties of well localized magnetic systems.

The temperature-dependent thermopower $S(T)$ is plotted in Fig. 9 for $Eu_yFe_{4-x}Co_xSb_{12}$. In the magnetically ordered range of the parent compound $Eu_{0.83}Fe_4Sb_{12}$, $S(T)$ is small and negative. The paramagnetic temperature range, however, is characterized by a positive, almost linear behavior, reaching about 50 μV/K around 300 K. A kink in $S(T)$ near 84 K also traces the phase transition temperature. Due to the Fe/Co substitution, magnetic ordering vanishes; hence the temperature range characterized by positive $S(T)$ values extends. Moreover, a significant increase of the absolute Seebeck coefficient is observed reaching for $Eu_{0.7}Fe_2Co_2Sb_{12}$ more than 100 μV/K at room temperature. However, on a further increase of the Co content, which is accompanied by a decrease of the content of electropositive Eu, $S(T)$ starts to reduce and eventually passes over to negative values. There,

a value as large as -110 μV/K is obtained for $Eu_{0.42}Fe_{0.6}Co_{3.4}Sb_{12}$. Measurements at higher temperatures for some of the compounds reveal values from 200 to -300 μV/K for $Eu_{0.7}Fe_2Co_2Sb_{12}$ and $Eu_{0.42}Fe_{0.6}Co_{3.4}Sb_{12}$, respectively. The overall behavior of $S(T)$ of $Eu_yFe_{4-x}Co_xSb_{12}$ can be referred to a change from a holelike (large Fe content) to electron-dominated transport (large Co content). In particular, and with respect to the stable binary semiconducting $CoSb_3$, $[Fe_4Sb_{12}]$ contains four holes. Charge is then carried primarily by these holes and the Seebeck coefficient becomes positive. According to the general formula of thermopower, i.e.,

$$S_d = \frac{\pi^2 k_B^2 T}{3|e|} \frac{1}{N(E_F)} \left(\frac{\partial N(E)}{\partial E} \right)_{E_F} \tag{1}$$

the energy derivative $dN(E)/dE$ for this scenario has to be negative, thus the density of states decreases near E_F. The holes created by $[(Fe,Co)_4Sb_{12}]$ are, at least partly, compensated by the electrons provided by the electropositive Eu. Since the parent material exhibits a Eu filling of $y=0.83$, a hole number slightly below 2 is evaluated as a rough approximation. Due to the Fe/Co substitution the hole number is reduced and further compensated by the electropositive element. The degree of filling of the voids in the skutterudite structure by Eu, however, simultaneously lowers. Beyond a critical Co concentration ($x \approx 3.5$), the carrier count yields a surplus of electrons, hence transport becomes electronlike. In fact, $S(T)$ of this specimen is negative in the whole temperature range. In the simple one-band model, the absolute value of the Seebeck coefficient depends on the carrier concentration.[34] As the carrier concentration decreases with the Fe/Co substitution, $S(T)$ grows, as evidenced by the experimental data. This prediction holds for both the hole and the electron dominated transport. As an implication, the Seebeck coefficient of $Eu_yCo_4Sb_{12}$ depends on the Eu concentration; i.e., for $y=0.2$, $S(T)$ is almost twice as large as the compound with $y=0.44$. The latter observation can serve to some extend as a justification of the simple carrier count performed above. However, Hall measurements carried out on pseudobinary $Co_{1-x}Fe_xSb_3$ demonstrated that the real carrier change due to the Co/Fe substitution is less than that derived above.[29] Nevertheless, even the simple arguments outlined seem to account for the evolution of the Seebeck coefficient and the change from hole- to electron-type transport throughout the whole series of $Eu_yFe_{4-x}Co_xSb_{12}$.

A study of the temperature-dependent thermal conductivity $\lambda(T)$ of $Eu_yFe_{4-x}Co_xSb_{12}$ is summarized in Fig. 10(a). Due to the strong interaction of the phonons with the weakly bound electropositive element, the lattice thermal conductivity of such skutterudite systems is strongly reduced and the theoretical minimum thermal conductivity, as found for glasslike materials, is almost reached. However, the well developed metallic conductivity of parent $Eu_{0.83}Fe_4Sb_{12}$ is responsible for a significant electronic contribution $\lambda_{el}(T)$ to the total measured quantity $\lambda(T)$. The observed absolute values are therefore larger than typically observed in this class of materials.[35] Quantitatively, a separation of $\lambda(T)$ into the

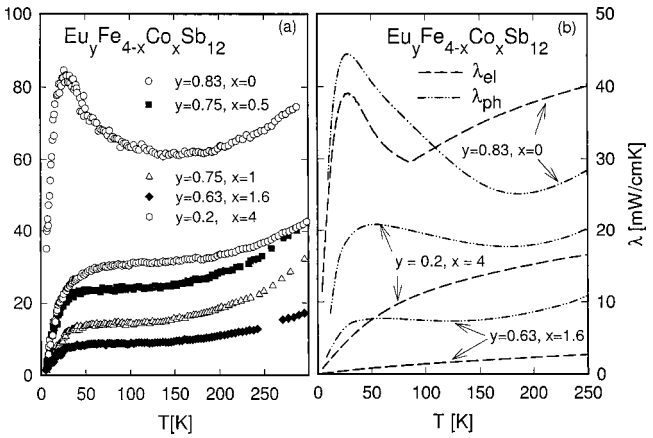

FIG. 10. (a) Temperature-dependent thermal conductivity λ of $Eu_yFe_{4-x}Co_xSb_{12}$ for various concentrations x. (b) Electronic part λ_e (dashed line) and lattice part λ_l (dashed-dotted line) of total thermal conductivity λ for $y=0.83$, 0.63, 0.20.

electronic part $\lambda_{el}(T)$ and the lattice part $\lambda_{ph}(T)$ can be derived from the Wiedemann Franz law. In the case of simple metals, the Wiedemann Franz law is expected to be valid, thus, $\lambda_{el}=L_0T/\rho$; $L_0=2.45\times10^{-8}$ W Ω K^{-2} is the Lorenz number and ρ is the electrical resistivity. Results of such an analysis are shown in Fig. 10(b) as dashed (λ_{el}) and dashed-dotted lines (λ_{ph}). Although the Wiedemann Franz law can serve just as a first approximation, the deduced results unambiguously point out that $\lambda_{el}(T)$ is non-negligible. Moreover, $\lambda_{el}(T)$ even exceeds $\lambda_{ph}(T)$ at elevated temperatures in the case of $Eu_{0.83}Fe_4Sb_{12}$. The importance of the electronic contribution to the total thermal conductivity in this particular case, most likely, originates from the significant number of uncompensated holes.

The effect of the Fe/Co substitution with respect to the thermal conductivity is initially a striking reduction of $\lambda(T)$. For the compound with $x=1.6$, λ at room temperature is already reduced to values as small as 18 mW/cm K. The application of the Wiedemann Franz law yields an electronic contribution of only 3 mW/cm K, thus reaching eventually 15% of the total measured effect. The observed thermal conductivity increase for the $y=0.2$ and $x=4$ sample is associated with the absence of crystal disorder and moreover, magnetic scattering processes are weakest within the series.

As already indicated in the previous section on thermopower, the carrier concentration is substantially reduced with the Fe/Co substitution. Within a simple single-band model, $\lambda_{el}(T)$ behaves proportional to the carrier concentration.[34] Hence, the observed diminishing of $\lambda_{el}(T)$ upon the Fe/Co substitution appears to be again a consequence of the substitution dependent decreasing number of free carriers.

The figure of merit ZT of $Eu_yFe_{4-x}Co_xSb_{12}$ with $Z=S^2/(\rho\lambda)$ was evaluated for those concentrations where thermal conductivity measurements were carried out. ZT smoothly increases with increasing temperature, ranging near room temperature from ZT=0.03 ($Eu_{0.75}Fe_{3.1}Co_{0.9}Sb_{12}$) to ZT$\approx$0.17 for $Eu_{0.2}Co_4Sb_{12}$.

IV. SUMMARY

Samples of the skutterudite-type solid solution $Eu_yFe_{4-x}Co_xSb_{12}$ were synthesized and found to be stable with Eu content significantly decreasing on increasing Fe/Co substitution from truly ternary $Eu_{0.83}Fe_4Sb_{12}$ to a mere solid solution of Eu in binary Co_4Sb_{12}. A variety of physical quantities was determined from L_{III}-XAS, ^{151}Eu-Mössbauer spectroscopy, magnetic studies, as well as measurements of transport coefficients (electrical resistivity, thermal conductivity, and thermopower) as a function of composition, temperature, pressure and magnetic fields. $Eu_{0.83}Fe_4Sb_{12}$ orders magnetically below $T_{mag}=84$ K; however, due to the Fe/Co substitution and concomitantly the reduction of the Eu content, long-range magnetic order becomes suppressed. The overall magnetic behavior in this series is not only determined from the moment bearing rare earth ion, rather, the $[(Fe,Co)_4Sb_{12}]$ sublattice substantially contributes to quantities such as the magnetic susceptibility and magnetization. Furthermore, owing to this substitution the valence state of Eu changes from magnetic $4f^7$ towards nonmagnetic $4f^6$. Mössbauer data in conjunction with the double-peak structure of the L_{III} spectra give evidence of the static admixture of the $4f^6$ and the $4f^7$ states of Eu in $Eu_yFe_{4-x}Co_xSb_{12}$. The Fe/Co substitution is accompanied by a significant change of the carrier concentration and drives electronic transport from hole to electron dominated conductivity as reflected from a crossover of the Seebeck coefficient from positive to negative signs. As a consequence of the decrease in the carrier density the absolute Seebeck values increase significantly, while the thermal conductivity lowers; thus the figure of merit enhances.

ACKNOWLEDGMENTS

This research was sponsored by the Austrian FWF under Grants No. P13778 and No. P12899 as well as by a grant for an international joint research project NEDO (Japan). The authors (C.G. and P.R.) are furthermore grateful for support by the Austrian-French Scientific-Technical exchange program Amadee 02587ZD. In the early stage of this research investigations were covered by the Austrian-Italian scientific-technical exchange program (A.S., N26) and some specific investigations were performed under the Austrian-Polish scientific-technical exchange program (D.K., P13/01).

[1] C. Uher, Semicond. Semimetals **69**, 139 (2001).
[2] E. Bauer, A. Galatanu, H. Michor, G. Hilscher, P. Rogl, P. Boulet, and H. Noel, Eur. Phys. J. B **14**, 483 (2000).
[3] E. Bauer, A. Galatanu, H. Michor, G. Hilscher, P. Rogl, P. Boulet, H. Noel, A. Grytsiv, and T. Velikanova, (unpublished).
[4] E. Bauer, St. Berger, A. Galatanu, H. Michor, Ch. Paul, G. Hilscher, V. H. Tran, A. Grytsiv, and P. Rogl, J. Magn. Magn. Mater. **226–230**, 674 (2001).
[5] E. Bauer, St. Berger, A. Galatanu, M. Galli, H. Michor, G. Hilscher, Ch. Paul, B. Ni, M. M. Abd-Elmeguid, V. H. Tran, A. Grytsiv, and P. Rogl, Phys. Rev. B **63**, 224414 (2001).
[6] M. E. Danebrock, Ch. H. B. Evers, and W. Jeitschko, J. Phys. Chem. Solids **57**, 387 (1996).
[7] W. Jeitschko, A. J. Foecker, D. Paschke, M. V. Dewalsky, Ch. B. H. Evers, B. Künnen, A. Lang, G. Kotzyba, U. Ch. Rodewald, and M. Möller, Z. Anorg. Allg. Chem. **626**, 1112 (2000).
[8] D. T. Morelli, G. P. Meissner, B. Chen, S. Hu, and C. Uher, Phys. Rev. B **56**, 7376 (1997).
[9] G. P. Meissner, D. T. Morelli, S. Hu, J. Yang, and C. Uher, Phys. Rev. Lett. **80**, 3551 (1998).
[10] F. Grandjean, G. J. Long, R. Cortes, D. T. Morelli, and G. P. Meisner, Phys. Rev. B **62**, 12 569 (2000).
[11] P. Duncumb and E. M. Jones (unpublished).
[12] J. Rodriguez-Carvajal, Physica B **192**, 55 (1992).
[13] A. Leithe-Jasper, D. Kaczorowski, P. Rogl, J. Bogner, W. Steiner, G. Wiesinger, and C. Godart, Solid State Commun. **109**, 395 (1999).
[14] A. Eiling and J. Schilling, J. Phys. F: Met. Phys. **11**, 623 (1981).
[15] W. Jeitschko and D. J. Braun, Acta Crystallogr., Sect. B: Struct. Crystallogr. Cryst. Chem. **33**, 3401 (1977).
[16] Yu. N. Grin, K. Hiebl, P. Rogl, and C. Godart, J. Alloys Compd. **239**, 127 (1996).
[17] D. Wohlleben, *Moment Formation in Solids*, edited by W. J. L. Buyers (Plenum, New York, 1984), p. 171.
[18] M. M. Abd-Elmeguid, Ch. Sauer, and W. Zinn, Phys. Rev. Lett. **55**, 2467 (1985).
[19] N. Lossau, H. Kierspel, J. Langen, W. Schlabitz, D. Wohlleben, A. Mewis, and Ch. Sauer, Z. Phys. B: Condens. Matter **74**, 227 (1989).
[20] N. Lossau, H. Kierspel, G. Michels, F. Oster, W. Schlabitz, D. Wohlleben, Ch. Sauer, and A. Mewis, Z. Phys. B: Condens. Matter **77**, 393 (1989).
[21] C. Godart, J. C. Achard, G. Krill, and M. F. Ravet-Krill, J. Less-Common Met. **94**, 177 (1983).
[22] E. Kemly, M. Croft, V. Murgai, L. C. Gupta, C. Godart, R. D. Parks, and C. V. Segre, J. Magn. Magn. Mater. **47**, 403 (1985).
[23] G. Michels, S. Junk, W. Schlabitz, E. Holland-Moritz, M. M. Abd-Elemeguid, J. Dünner, and A. Mewis, J. Phys.: Condens. Matter **6**, 1769 (1994).
[24] M. M. Abd-Elmeguid, H. Miklitz, and G. Kaindl, Phys. Rev. B **23**, 75 (1981).
[25] A. Gerard, F. Grandjean, J. Hodges, D. J. Braun, and W. Jeitschko, J. Phys. C **16**, 2797 (1983).
[26] H. Harima, Prog. Theor. Phys. Suppl. **138**, 117 (2000).
[27] E. Bauer, St. Berger, A. Galatanu, Ch. Paul, M. Della Mea, H. Michor, G. Hilscher, A. Grytsiv, P. Rogl, D. Kaczorowski, L. Keller, T. Herrmannsdörfer, and P. Fischer, Physica B **312-313**, 840 (2002).
[28] G. J. Long, D. Hautot, F. Grandjean, D. T. Morelli, and G. P. Meissner, Phys. Rev. B **60**, 7410 (1999).
[29] J. Yang, G. P. Meisner, D. T. Morelli, and C. Uher, Phys. Rev. B **63**, 014410 (2001).
[30] D. J. Singh and I. I. Mazin, Phys. Rev. B **56**, R1650 (1997).

[31] V. L. Kuznetsow and D. M. Rowe, J. Phys.: Condens. Matter **12**, 7915 (2000).
[32] G. T. Meaden, Contemp. Phys. **12**, 313 (1971).
[33] C. Huhnt, G. Michels, W. Schlabitz, D. Johrendt, and A. Mewis, J. Phys.: Condens. Matter **9**, 9953 (1997).
[34] C. M. Bhandari, in *CRC Handbook of Thermoelectrics*, edited by D. M. Rowe (CRC, Boca Raton, 1995), p. 55.
[35] B. C. Sales, D. Mandrus, B. C. Chakoumakos, V. Keppens, and J. R. Thompson, Phys. Rev. B **56**, 15 081 (1997).